Iran J Sci Technol Trans Mech Eng (2019) 43:127–138
DOI 10.1007/s40997-017-0119-8

RESEARCH PAPER

Simulation of Composite Laminate with Cohesive Interface Elements Under Low-Velocity Impact Loading

Enock A. Duodu[1] · Jinan Gu[1] · Wei Ding[1] · Zhenyang Shang[1] · Shixi Tang[1]

Received: 9 December 2016 / Accepted: 21 October 2017 / Published online: 6 November 2017

Abstract In this paper, numerical model based on continuum damage mechanics is presented to predict the damage behavior in quasi-isotropic composite laminates under low-velocity impact conditions. Hashin criterion and a gradual degradation scheme are employed to trigger the intra-laminar damage initiation and growth. Additionally, an interface cohesive element is incorporated in the model to predict the inter-laminar delamination damages. A user-defined subroutine VUMAT comprising these constitutive models of intra-laminar and inter-laminar damage is written in FORTRAN and implemented into explicit finite element package ABAQUS. Parametric analysis is performed on quasi-isotropic composite model with different impact energy levels to study the impact velocity–time, velocity–displacement, acceleration–time and acceleration–displacement curves of full and reduced models as well as the damage development of intra-laminar matrix cracking and inter-laminar delamination. Reasonable accord between the numerical simulations and experimental test indicates good prediction of impact damage behavior of the proposed model at low-velocity impact conditions.

Keywords Cohesive element · Cross-ply composite · Finite element model · Low velocity · Quasi-isotropic composite

✉ Enock A. Duodu
enockduodu@ujs.edu.cn

[1] School of Mechanical Engineering, Jiangsu University, Zhenjiang 212013, Jiangsu, China

1 Introduction

Composite materials have replaced traditional materials in the application of structures such as aerospace, marine, civil and automotive fields due to their high excellent properties and long service life. In aviation industry, composites are believed to have superior potential applications as the main load-bearing structure. However, these materials are poor to impact resistance owing to loading conditions, which results in poor damage resistance. Failure of composite material under low velocity is a complex process involving intra-laminar and delamination damages leading to reduction in stiffness and strength properties. Generally, damage in solid laminated composite under low impact velocity reduces the residual structural mechanical performance. Based on this, study on impact response of composite laminates in the design of aviation structures and structural components is very important.

Today, studies on impact behavior of composite laminates have been covered in numerous reviews. Choi et al. (2010) have used a displacement field plate theory to investigate low-velocity impact response in composite laminates under in-plane loads. It found that the tensile and compressive loads as well as the damage areas were compared well with experimental test for different impact energy levels. Xiao et al. (2014) carried out an analytical method to predict the damage area on composite laminates induced with low-velocity impact. It establishes that the maximum contact force and initial inter-laminar shear strength based on Eshelby's equivalent definition agree well with physical test result. Olsson (2001) proposed a model to predict the impact damage initiation and growth during quasi-static impact response with large mass impactors and found that the residual bending stiffness degradation is relevant in all layups and boundary

conditions. Hosur et al. (2005) carried out experimental study to determine the impact response of four different hybrid laminates subjected to low-velocity loading conditions. It found that the hybrid composites are slightly stiffer than glass/epoxy and carbon/epoxy composite laminates.

Zhang et al. (2013) have carried out experimental test to predict the damage behavior under low velocity in three different kinds of composite laminates. The result shows that the effect of single-layer fabric structure exhibits better impact performance and delamination resistance compared with the others. Sevkat et al. (2013) carried out empirical studies on hybrid reinforced composite laminates to predict the damage threshold under low velocity. The result shows that impact performance is significantly affected by the nylon/basalt fiber content. Also, experimental analysis of low-velocity impact on woven carbon composite is performed (Soliman et al. 2012), and study reveals that MWCNTs enhance the impact response resulting in lesser damage area. Mitrevski et al. (2006) have performed a physical experimental test to predict the influence of impactor shape and tensile biaxial preload on the impact response of thin glass fiber-reinforced polyester laminated composite. Result observed that the contact force, impact energy and damage area remain the same during preloading conditions.

Recently, many numerical studies have been done on impact structures of composite laminates. Lopes et al. (2009a, b) have used experimental and simulation model to predict damage on multi-directional composite laminates at low-velocity impact. Their study shows that the largest delamination occurs at the innermost interface leading to reduction in the residual compressive strength of the composite material. Zhang et al. (2012a) employed simulation model to analyze the low-velocity impact damage on composite plate where cohesive elements are introduced at the interface. Similarly, Feng and Aymerich (2014) have numerically predicted the structural impact response of laminated composites with interface cohesive elements under low-velocity impact. The study presents an accurate prediction of the structural behavior for different impact energy levels.

Even though many numerical models have been established to track the impact response on the interface architecture in composite laminates (Jang et al. 2017; Zhang and Zhang 2015; Kumar et al. 2016; Shi and Soutis 2016; Lachaud et al. 2015), yet further studies on carbon fiber-reinforced epoxy are necessary for efficient application in aero-structures. Owing to this importance, researchers have adopted two techniques to enhance interface damage prediction in composite laminates, including virtual crack closure-integral technique (VCCT) and cohesive zone model (CZM). However, VCCT cannot predict crack initiation and need additional adaptive re-meshing technique for delamination. Alternatively, CZM uses strength-based and fracture energy criteria to predict damage initiation and evolution, which overcomes the limitations in VCCT framework. As a result, the CZM-based interface elements have attracted much attention in the simulation of delamination and matrix cracking modes in the damaged composite laminates (Bouvet et al. 2009; Shi et al. 2014a, b; Liu et al. 2015; Long et al. 2015; May 2015; Kumar et al. 2016; Li et al. 2008; Zhang et al. 2012b). On this note, surface-based cohesive contact model is adopted to trigger inter-laminar impact response due to the advantage of predicting damage initiation and evolution without previous knowledge of crack location and propagation direction.

In this study, a 3D finite element model based on continuum mechanics is established to predict damage response in quasi-isotropic composite laminate under low-velocity impact loading condition. The formulated constitutive models are applied into ABAQUS/Explicit solver through the user-defined subroutine VUMAT, written in FORTRAN. In addition, cohesive elements are introduced at the inter-laminar interfaces to activate damage initiation and growth. Analysis of the model is discussed in detail, and numerical predictions are found to be in acceptable agreement with the experimental data to validate the efficiency and dependability of the proposed simulation model.

2 Damage Modeling

Matrix cracking, fiber breakage and delamination are the main failure modes in composite laminates under low-velocity loading condition. The impact damage process can be activated with damage models consisting of damage initiation criterion and damage evolution law.

2.1 Intra-laminar

In this study, damage model based on continuum damage mechanics (CDM) where internal state variables are used as coefficients to activate intra-damage development is chosen. The famous Hashin failure criteria described in reference of Zhang and Zhang (2015) are chosen to track intra-laminar matrix and fiber damages and summarized as follow:

Tensile matrix cracking

$$\left(\frac{\sigma_{22}}{Y_{\mathrm{T}}}\right)^2+\left(\frac{\tau_{12}}{S_{12}}\right)^2+\left(\frac{\tau_{23}}{S_{23}}\right)^2 \geq 1 \tag{1}$$

Compressive matrix cracking

$$\left(\frac{\sigma_{22}}{Y_{\mathrm{C}}}\right)^2+\left(\frac{\tau_{12}}{S_{12}}\right)^2+\left(\frac{\tau_{23}}{S_{23}}\right)^2 \geq 1 \tag{2}$$

Tensile fiber failure

$$\left(\frac{\sigma_{11}}{X_T}\right)^2+\left(\frac{\tau_{12}}{S_{12}}\right)^2+\left(\frac{\tau_{23}}{S_{23}}\right)^2\geq 1 \quad (3)$$

Compressive fiber failure

$$\left(\frac{\sigma_{11}}{X_T}\right)^2+\left(\frac{\tau_{12}}{S_{12}}\right)^2+\left(\frac{\tau_{23}}{S_{23}}\right)^2\geq 1 \quad (4)$$

Fiber–matrix shear-out

$$\left(\frac{\sigma_{11}}{X_C}\right)^2+\left(\frac{\sigma_{12}}{S_{12}}\right)^2+\left(\frac{\sigma_{23}}{S_{23}}\right)^2\geq 1 \quad (5)$$

To satisfy the intra-laminar failure criteria for damage evolution, material degradation rule (Zhang and Zhang 2015) is applied to degrade the structural stiffness of the material properties in order to compute the actual impact threshold. The degradation material properties are listed in Table 1.

Where σ_{11} and σ_{22} are the in-plane stresses in the fiber and transverse directions, τ_{12} and τ_{23} represent the shear stresses, X_T and X_C refer to the fiber tension and compression strengths, Y_T and Y_C are the matrix tension and compression strengths, S_{XY} is the fiber–matrix shear-out, S_{12} and S_{23} denote the shear strengths, and 'd' refers to the degraded material properties. The E and G denote allowable elastic and shear modulus, respectively.

2.2 Inter-laminar Damage

The cohesive zone elements are adopted to simulate the inter-laminar delamination behavior at the interfaces of adjacent layers in the composite laminates. The traction stress and separation displacement of the nodes on the interface are governed by traction–separation model consisting of damage initiation criterion and damage evolution law. Actually, delamination propagation is likely to take place under mixed-mode loading; thus, delamination initiation and the corresponding reduction behavior are determined by damage modes I, II and III simultaneously. For the mixed-mode loading, the current effective relative displacement, δ_m, is introduced as

$$\delta_m=\sqrt{\langle\delta_1\rangle^2+\delta_2^2+\delta_3^2} \quad (6)$$

where the symbol $\langle\ \rangle$ represents the Macaulay operator.

For a linear reduction process, the damage variable d for damage evolution is expressed by

$$d=\frac{\delta_m^f\left(\delta_m^{\max}-\delta_m^0\right)}{\delta_m^{\max}\left(\delta_m^f-\delta_m^0\right)} \quad (d\in[0,1]) \quad (7)$$

where δ_m^0 and δ_m^f are the effective relative displacements of interface at damage initiation and complete failure; and the maximum current relative displacement $\delta_m^{\max}$ is defined as $\delta_m^{\max}=\max\left\{\delta_m^{\max},\ \delta_m\right\}$ regarding the damage irreversibility.

A quadratic stress criterion is used to determine the damage initiation displacement, i.e., δ_m^0, of the interface, which is given by

$$\left(\frac{\sigma_n}{N}\right)^2+\left(\frac{\sigma_s}{S}\right)^2+\left(\frac{\sigma_t}{T}\right)^2\geq 1 \quad (8)$$

where, N, S and T represent the interface strengths in the normal and shear directions, respectively, and σ_n, σ_s and σ_t are the corresponding interface stresses.

For damage evolution under mixed-mode loading, Benzeggagh–Kenane fracture energy criterion (Bui 2011) which describes the variation of fracture energy within cohesive elements is adopted and expressed by the relation.

$$G=G_{IC}+(G_{IIC}-G_{IC})\left(\frac{G_{shear}}{G}\right)^{\eta} \quad (9)$$

Herein, $G_{shear}=G_{II}+G_{III}$ is the energy release rate for mixed-mode shear loading. G_I, G_{II}, G_{III} are the strain energy release rates under the modes I, II and III, respectively. G_{IC}, G_{IIC} and G_{IIIC} are the critical strain energy release rates. The exponent η is the cohesive coefficient, and G is the critical strain energy release rate of the cohesive element.

Finally, a FORTRAN pre-compiler code comprising these constraint relations are written and implemented in the damage model based on the platform of finite element software ABAQUS/Explicit (Systèmes, S-D 2011a).

Table 1 Material property degradation rule

Failure mode	X_T	X_C	Y_T	Y_C	S_{XY}
Degradation law	$E_{11,d}=0.7E_{11}$	$E_{11,d}=0.14E_{11}$	$E_{22,d}=0.2E_{22}$ $G_{12,d}=0.2G_{12}$ $G_{23,d}=0.2G_{23}$	$E_{22,d}=0.4E_{22}$ $G_{12,d}=0.4G_{12}$ $G_{23,d}=0.4G_{23}$	$G_{12,d}=0$ $v_{12,d}=0$

3 Finite Element Model

3.1 Geometry Modeling and Boundary Condition

A carbon fiber/epoxy laminated composite plate of radius 50 mm and thickness 4 mm is designed with the aid of ABAQUS/Explicit software. Firstly, a cross-ply model of stacking sequence $[-45/0/45/90]_{4S}$ is constructed to validate the model. Also, two models with stacking configuration of $[90_4/0_2/90_4]$ and $[90/45/45/0/-45]_S$ are established for impact damage analysis. In the models, fixed boundary conditions are fully assigned to the circumferential edge of the composite plate. The impactor is modeled as a rigid spherical body of mass 6.8 kg and radius 7.88 mm. The impactor is prescribed in the z-direction with all degree of freedoms constrained to zero replicating physical test conditions as described in reference of Khalili et al. (2011).

3.2 Types of Finite Element Used and Mesh Density

A solid continuum (C3D8R) element and cohesive (COH3D8) formulations are incorporated into the model to simulate damage formation. Each ply of the laminated plate is modeled with eight node elements with three degrees of freedom for each node and a reduced integration arrangement. Hashin failure criterion is applied for intra-laminar damage based on continuum damage mechanics approach to consider the material degradation properties as previously described. Surface-based cohesive contact model of zero thickness is employed between layers with different fiber orientations to trigger delamination initiation and propagation using quadratic stress-based criterion and the interactive mixed-mode Benzeggagh–Kenane fracture energy criterion, respectively. Failed cohesive elements are allowed to remain in the model to avoid penetration between delaminated layers. Fine mesh of size (0.5 mm × 0.5 mm) is assigned in the impact zone where damage is envisaged, while a sizeable coarse mesh is employed outside the impact region. The composite laminate is meshed with a total of 27,880 solid elements, 57,140 nodes and 25,092 cohesive elements for simulation analysis.

3.3 Contact Algorithm and Material Properties

The contact properties are considered to be hard (Khalili et al. 2011); therefore, the interaction between the composite plate and the impactor is simulated by surface-to-surface contact pairs within ABAQUS/Explicit platform which uses penalty enforcement contact method (Systèmes, S-D 2011b). The impactor is considered as master and the contact surface of the laminated composite plate as slave surface as in reference of Khalili et al. (2011) Carbon fiber/epoxy composite laminates of different stacking orientations are employed for analysis. The cohesive element parameters and material properties of the composite laminates (Zhang and Zhang 2015; Shi et al. 2012) used in the study are listed in Tables 2 and 3.

3.4 Computational Analysis

The user-defined FORTRAN subroutine (VUMAT) pre-compiler program which implements continuum damage model and inter-laminar failure criterion based on the platform of finite element software ABAQUS/Explicit as mentioned earlier is implemented for the impact simulation analysis.

Table 2 Cohesive element parameters

K_N (N/mm^3)	$K_S = K_T$ (N/mm^3)	N (MPa)	$S = T$ (MPa)	G_{IC} (N/mm)	$G_{IIC} = G_{IIIC}$ (N/mm)	Density (kg/m^3)	η
2.4×10^5	8.6×10^4	64	121	0.32	0.58	1600	2

Table 3 Material properties used in the models

Density (kg/m^3)	1600
Stiffness properties	$E_{11} = 162$ GPa; $E_{22} = E_{33} = 8.34$ GPa; $v_{12} = v_{13} = v_{23} = 0.27$ $G_{12} = G_{13} = G_{23} = 4.96$ GPa
Strength properties (MPa)	$X_T = 2275$; $X_C = 1680$; $Y_T = 64$; $Y_C = 186$; $S_{12} = 121$; $S_{13} = S_{23} = 127$
Fracture energy (N/mm)	$G_{ft} = 91.6$; $G_{fc} = 79.9$; $G_{mt} = 0.22$; $G_{mc} = 1.1$

4 Results and Discussion

A numerical result obtained from the model is discussed to validate the model with the experimental test parameters. The impact damage variables of full and reduced models such as velocity, acceleration and displacement with corresponding impact energy levels are compared. A parametric analysis with respect to damage size at the top and bottom surfaces of the proposed model is also presented.

4.1 Validation of the Model

Experimental test and simulation data in reference of Zhang and Zhang (2015) are used to validate the present numerical model with impact energy levels of 10 and 20 J. Figure 1 illustrates the impact force–time for the present numerical as well as the reference experimental and simulation results. It is observed that the present model agrees excellently with the result from reference. It can be seen that during the damage development, the numerical models slightly diverge from the experimental test, particularly, during the impact energy level of 10 J. The discrepancy may arise due to approximation in the failure criteria of the model. It is also observed that all the impact energy levels display similar damage characteristics curve with load increases swiftly to maximum during initiation before declines for propagation. This rapid load drop-off shows the maximum limit of residual stress carrying capacity of the composite laminate. The reason may be necessitated by inter-laminar interaction of layers after degradation of material properties in the model. The threshold load failure

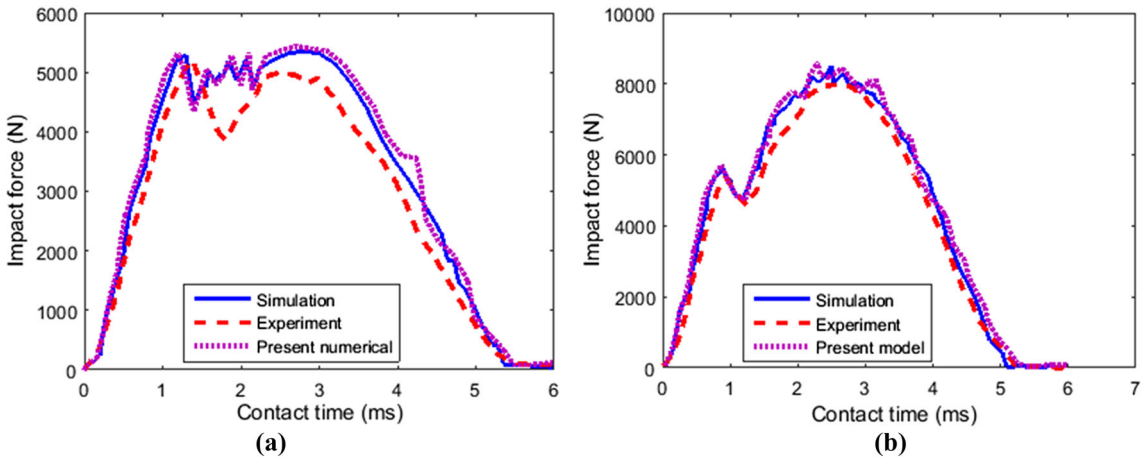

Fig. 1 Comparison of present model and reference results of contact force versus time for different energy levels. **a** 10 J. **b** 20 J

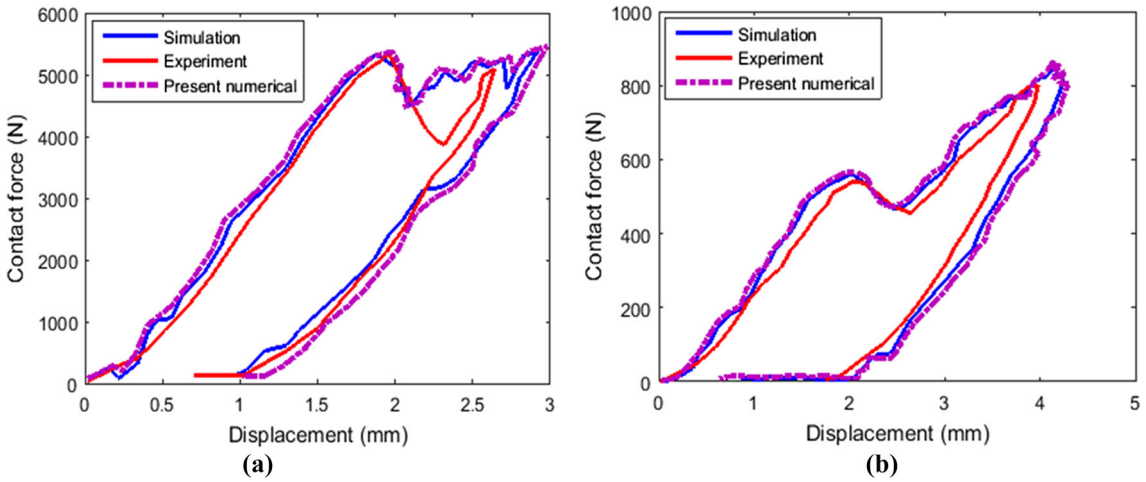

Fig. 2 Comparison of present model and reference data of contact force versus displacement for different energy levels. **a** 10 J impact energy. **b** 20 J impact energy

can also be attributed to the bending response as the laminate absorbs impact energy in the form of flexural stresses.

Figure 2 presents the impact force against displacement of the present numerical model and reference experimental and simulation data. Again, a good match between the models and experimental test is achieved for all the impact energy levels. When the impact energy reaches the maximum value, the impact velocity of the impactor turns to zero. After that, the elastic energy of the laminates drives the impactor for rebound. However, marginal realistic differences are observed between the models and the physical test which may occur due to excessive contact pressure between the impactor and composite laminate plate, thus resulting in matrix cracking and fiber braking as well as debonding of matrix–fiber interfaces. This contact pressure presumably creates damage due to friction between the impactor and the composite laminate leading to increase in the impact duration. This shows that decrease in impact load creates higher contact area with shear stresses triggering delamination damage. It is also seen that the area under the curves represents damage initiation and growth in the laminated composite plate. It is evident that the numerical results emphasize the need to incorporate cohesive interface elements in the damage models to track delamination development.

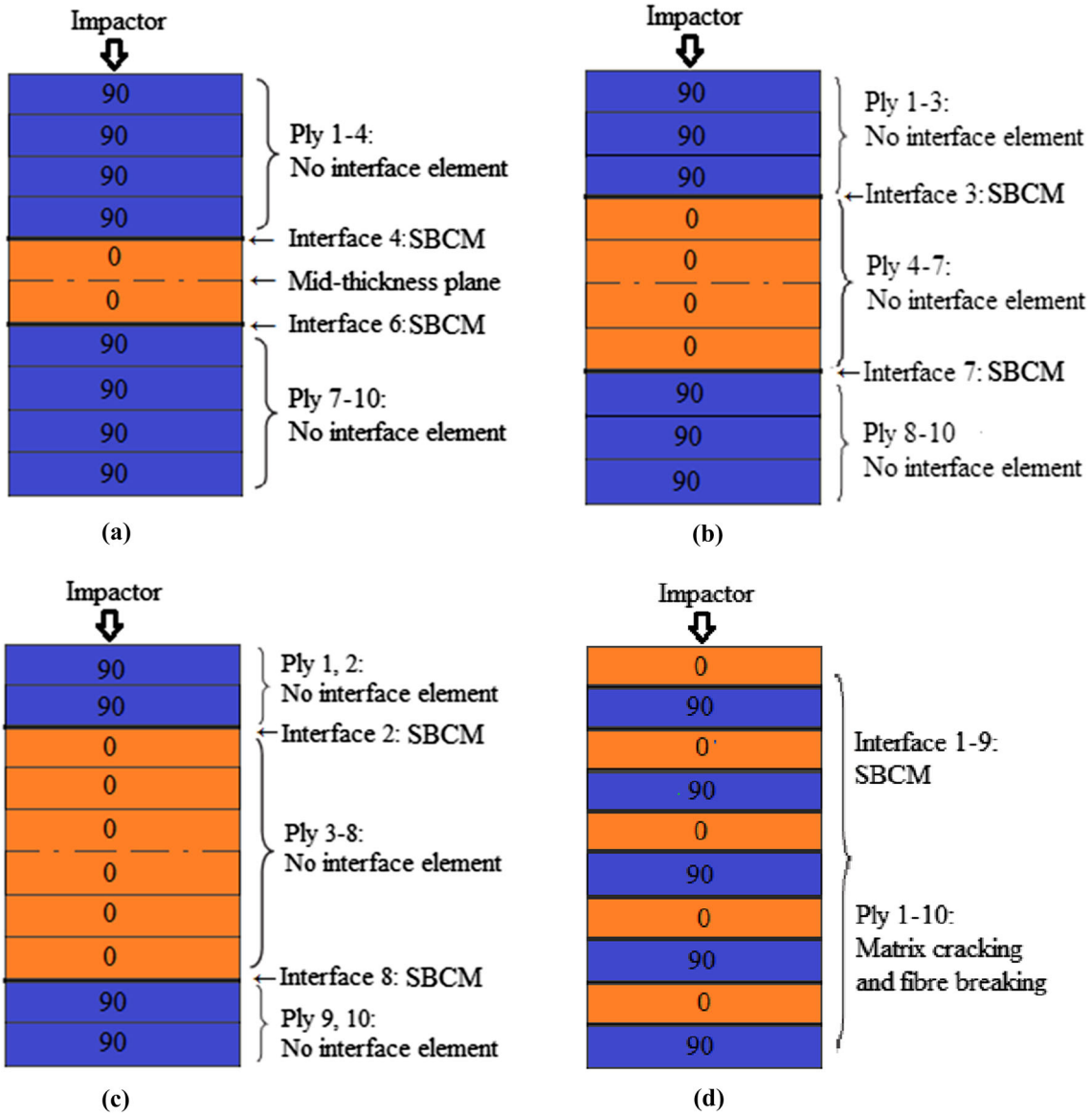

Fig. 3 Interface element definition for the cross-ply models. **a** Model 1, **b** Model 2, **c** Model 3, **d** Model 4

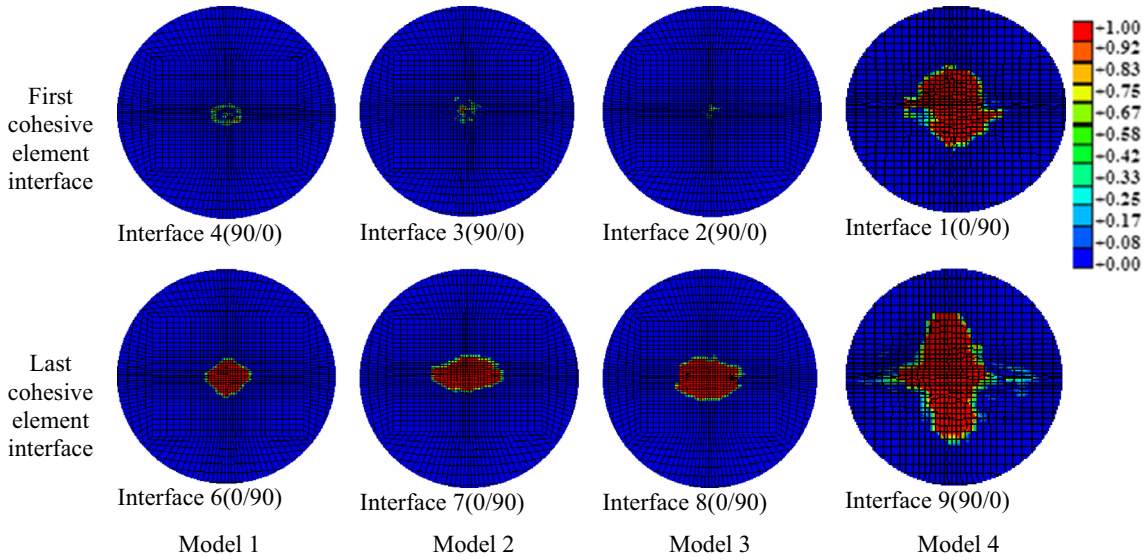

Fig. 4 Comparison of delamination areas in typical interfaces for the cross-ply models at impact energy level of 10 J

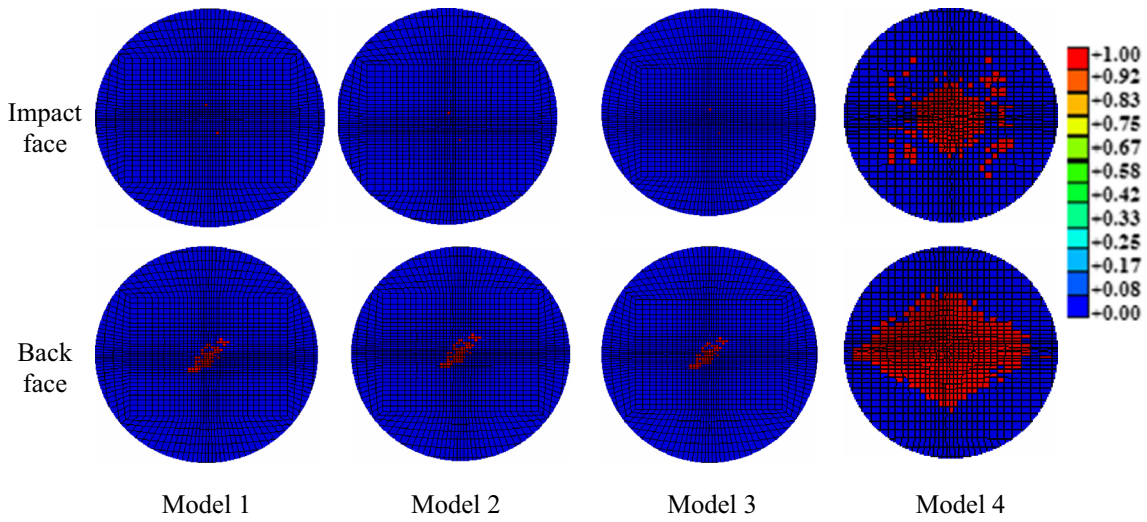

Fig. 5 Matrix cracking on front and back surfaces for the cross-ply models at 10 J impact thresholds

4.2 Impact Damage Response of the Cross-ply Models

In Fig. 3, cohesive interface elements are introduced at the interfaces between plies of different fiber orientation to trigger delamination damage initiation and progression. Since no delamination is envisaged in fibers with same ply orientations, no interface element is utilized. As shown in Model 1 of Fig. 3a, cohesive interface elements are inserted only at interfaces 4 (90/0) and 6 (0/90) near the mid-thickness plane. In Model 2 of Fig. 3b, cohesive interface elements are placed between interfaces 3 (90/0) and 7 (0/90). Also with Model 3, cohesive interface elements are introduced in the 2nd (90/0) and 8th (0/90) interfaces as shown in Fig. 3c. From the diagram in Fig. 3d, cohesive interface elements are introduced between all the layers (interfaces 1–9). Naturally, in Models 1–3 no fiber breaking and matrix cracking occur on the interfaces with same ply configuration. However, matrix cracking, fiber breaking and fiber–matrix debonding are anticipated on layers with different ply orientations. In Model 4, damage is predicted on each of the layers and interfaces in the form of matrix cracking, fiber breaking and delamination due to reduction in stiffness and strength of the composite laminates.

Figure 4 compares delamination shapes of typical interfaces in the cross-ply models under impact energy level of 10 J. The images show that the largest damage threshold occurs in Model 4, while the least damage area is

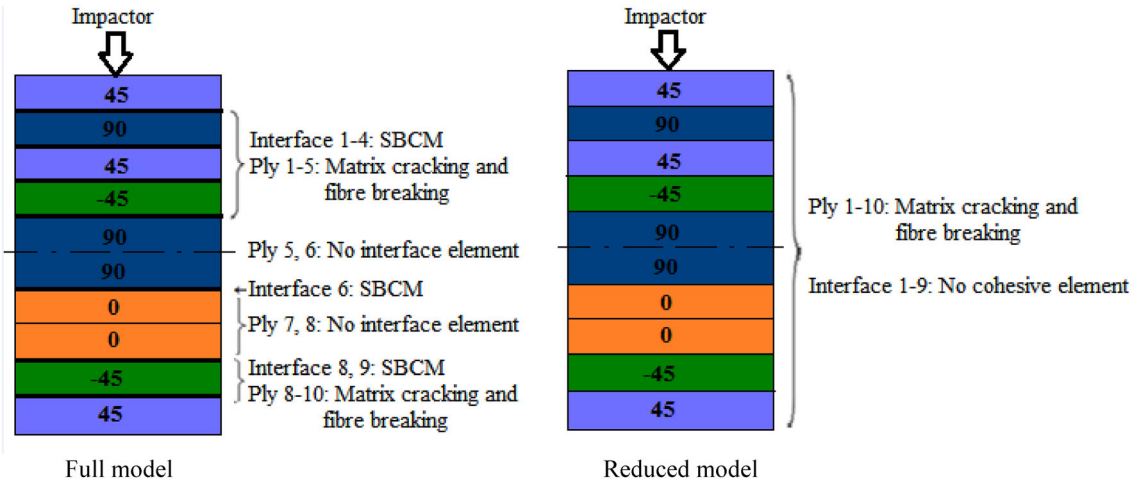

Fig. 6 Interface element definition of models

predicted in Model 3. It can also be seen that the bottom interfaces had the greatest delamination shape compared to the top interfaces. This phenomenon may be attributed by long contact duration between the impactor and the bottom layer of the composite laminate. Also, it can be attributed to the bending response as the laminate absorbs impact energy in the form of flexural stresses.

Figure 5 shows the comparison of matrix cracking development on the top and bottom layers under impact energy regime of 10 J. The numerical simulation results show that the damage area of fiber breaking is insignificant in the composite laminates under this impact energy level; however, matrix cracking can be found on each layer. It can be observed that the matrix cracking on the impact face registered small damage contour except in Model 4 where excessive damage is generated. Contrary, the bottom surface experiences considerable damage area as observed in Model 4. It is also observed that small amount of matrix damage tracking from the top plies through to the bottom ply where extensive deformation occurs. This establishes that damage threshold becomes wider as the impact threshold increases for all the damage models.

4.3 Numerical Analysis of Quasi-Isotropic Model

In this study, full model is described as a model where cohesive interface elements are placed at the interfaces between plies of different fiber orientation. With the full model, both inter-laminar and intra-laminar failure criteria are used to address the impact damage responses. On the other hand, reduced model is defined as a model with no cohesive element inserted between plies interfaces irrespective of fiber configuration. Herein, no inter-laminar debonding is expected occurring; thus, only intra-laminar failure criteria are adopted to track damage mechanisms. Based on the applicability of the cross-ply models, an explicit finite element model is established to predict the impact response of multi-directional composite laminate as shown in Fig. 6. As already defined, full model (Fig. 6a) and reduced model (Fig. 6b) are compared for simulation analysis. In the full model, fiber breaking and matrix cracking are envisaged to occur in plies 1–5 and plies 8–10 on the top and bottom layers, respectively; thus, cohesive elements are inserted at the interfaces 1–4, 6, 8 and 9 using the surface-based contact model to track delamination initiation and propagation. Since no delamination is anticipated between fibers of the same orientation, no interface element is placed between (90/90) and (0/0) interfaces. In the reduced model per the definition, no interface cohesive element is considered in the model at all.

4.3.1 Numerical Simulation Delamination Area and Matrix Cracking

A predicted delamination shape of selected interfaces on the impact zone for the three impact energy levels is presented in Fig. 7. Delamination occurs first in the upper interfaces and continues through the remaining cohesive interfaces. It can be seen that delamination area propagates toward the edges of the composite plate from the impact zone. Also, damage size orients parallel to the direction of the fiber stacking sequence. In comparison, the largest delamination is predicted on the 6th interface (90/0) which is very close to the mid-plane of the composite plate. The smallest delamination area is visualized on the 9th interface (− 45/45) near the bottom layer. Delamination is presumably provoked by the onset of fiber damage which happens concurrently with matrix cracking. Thus, it is assumed that delamination is the main damage mode in

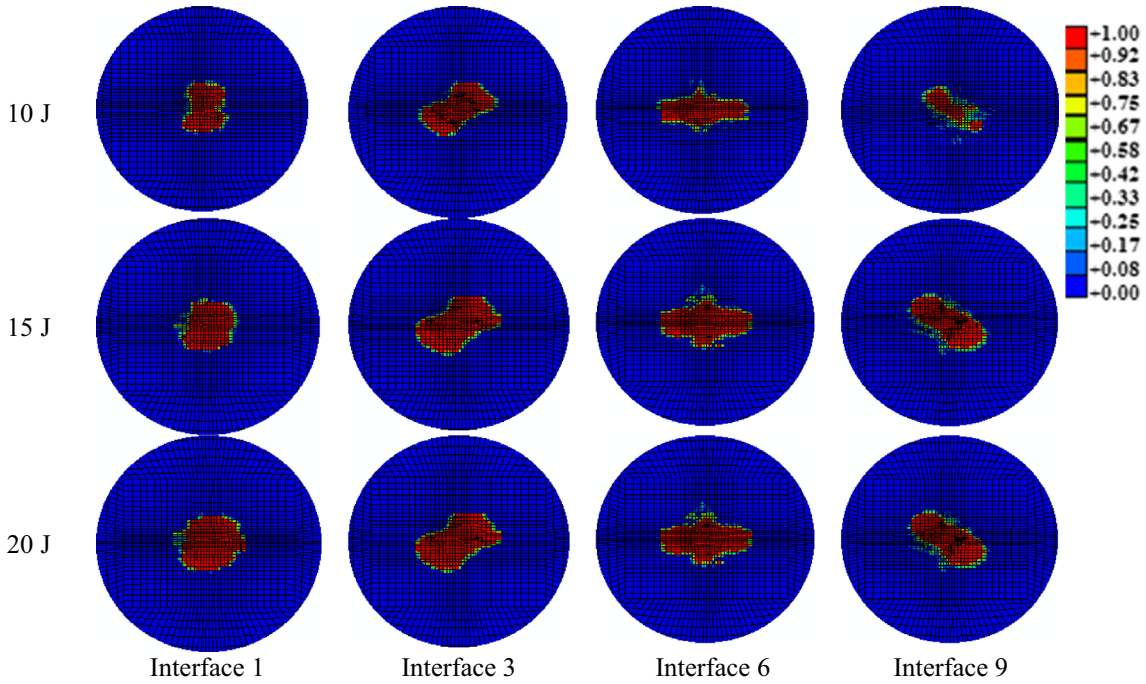

Fig. 7 Predicted delamination shape of selected interfaces for different impact energy levels

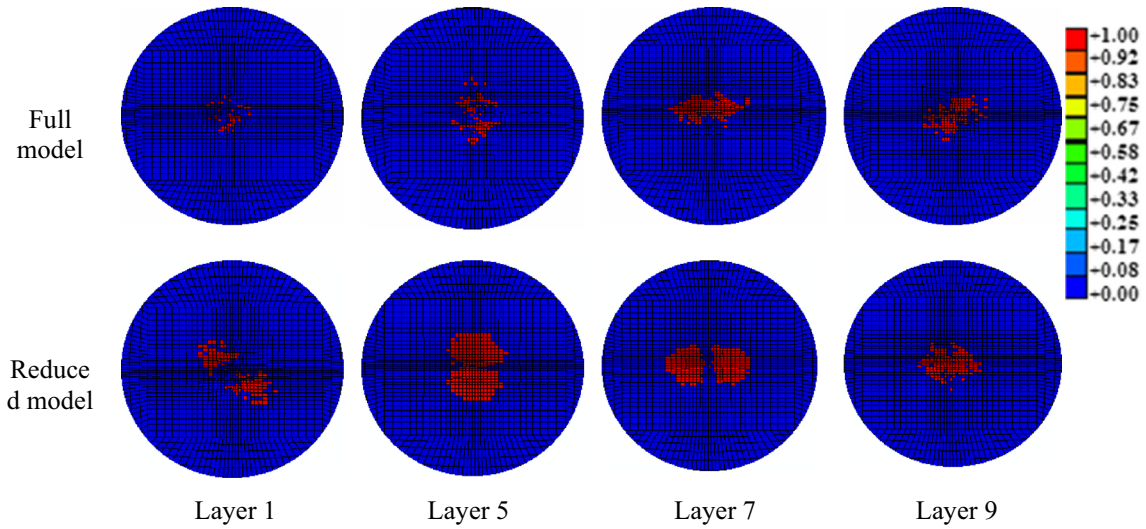

Fig. 8 Matrix cracking of typical layers for the full and reduced models under impact energy level of 10 J

composite laminate which causes degradation in material mechanical properties due to stress concentration between the inter-laminar surfaces. It is also realized that delamination area increases with increase in impact energy levels. In assessing delamination under different energy levels, it can be resolved that the higher the impact energy, the larger the damage area of matrix cracking. Moreover, the extent of damage tilts along the thickness direction and basically similar.

Figure 8 shows the matrix cracking on the typical layers of the models under impact energy threshold of 10 J. Once again, the simulation result shows that the damage size of intra-laminar fiber breakage is insignificant under this impact energy threshold on the composite laminates, but matrix cracking can be observed on each layer. It can be seen that the reduced model predicted large matrix cracking compared to the full model. This perhaps may be ascribed to the absence of interface cohesive elements in the reduced model. It can also be seen that the smallest matrix cracking is found on the 1st layer, followed with 9th layer, while the largest damage is predicted on the 5th layer. The damage discrepancy between the models is

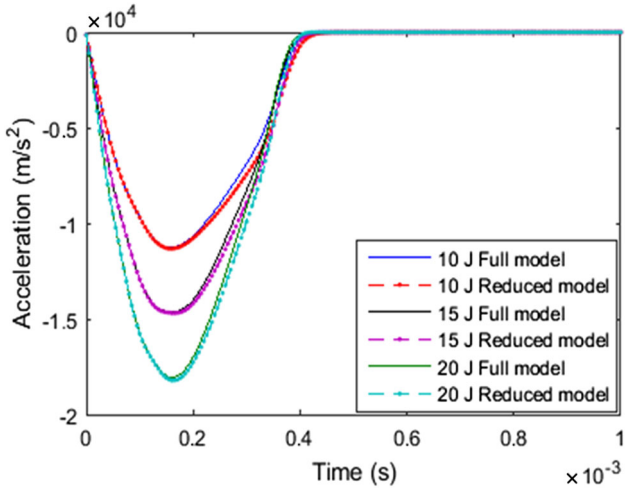

Fig. 9 Comparison of model acceleration–time curves for different impact energy levels

significant showing that failure on the composite laminate occurs as a result of excessive elastic deformation and bending response which leads to induced damage. It is evident that the obtained numerical results emphasize the need to incorporate cohesive interface elements in the damage model to track delamination development.

4.3.2 Numerical Simulation Analysis Curves

Figure 9 shows the acceleration–time histories of the models for different impact energy levels. It can be seen from the plot that retardation rate triggers downward immediately after initiation to about 11.28×10^3 m/s^2 within 0.16 ms and rebounds swiftly to reach zero acceleration at 0.49 ms via the application of the full model, whereas the reduced model also moves downward to a peak retardation rate of 11.33×10^3 m/s^2 within the same contact duration and rebounds quickly to complete the event at 0.55 ms during the 10 J impact energy. Similar and consistent trends are predicted for both 15 and 20 J impact energy levels, where an average maximum retardation rate is about 14.6×103 and 18.2×10^3 m/s^2 within the same duration, respectively. The sharp drop-off shows the maximum limit of residual stress carrying capacity of the composite laminate. The reason may be necessitated by inter-laminar interaction of the layers after degradation of material mechanical properties. Good agreement is observed between the full and reduced models, with peak retardation difference of $< 1\%$.

Acceleration–displacement comparison curves for impact energy levels of 10, 15 and 20 J are presented in Fig. 10 for the reduced and full models. The curves show a reasonable match between the energy levels during impact development. For instance in the 10 and 20 J impact test of the full model, a respective maximum deceleration of 11.3×10^3 and 18.1×10^3 m/s^2 with a corresponding displacement of 0.40×10^{-3} and 0.57×10^{-3} m is numerically predicted. For the reduced model on the other hand, maximum decelerations of approximately 11.3×103 and 18.2×103 m/s^2 with the same displacement levels are observed. Comparable and consistent threshold is observed in the 15 J impact energy test. The parabolic curve symbolizes damage initiation and progression in the composite plate. With the increase in acceleration, the composite laminates absorb more energy, which means that the damage situation becomes more severe.

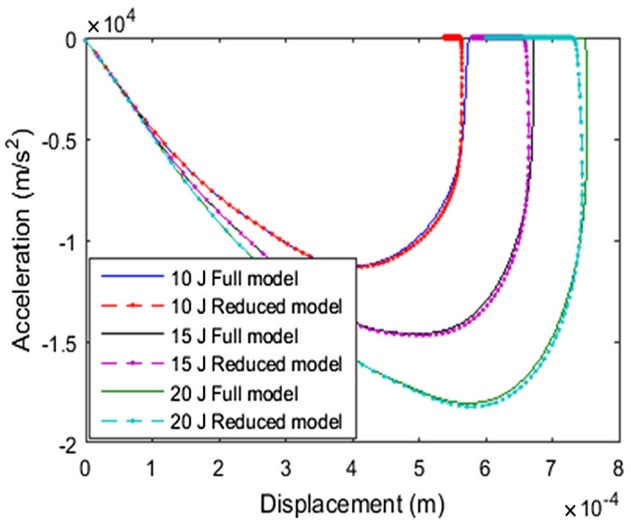

Fig. 10 Acceleration versus displacement response of the model for different impact levels

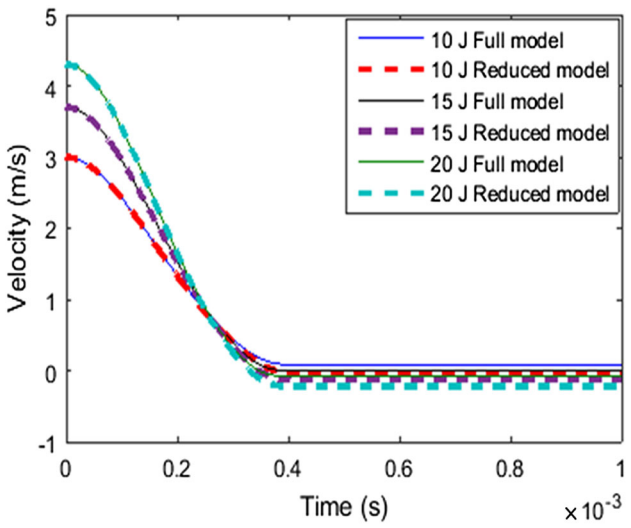

Fig. 11 Comparison of model velocity–time curves for different impact energy levels

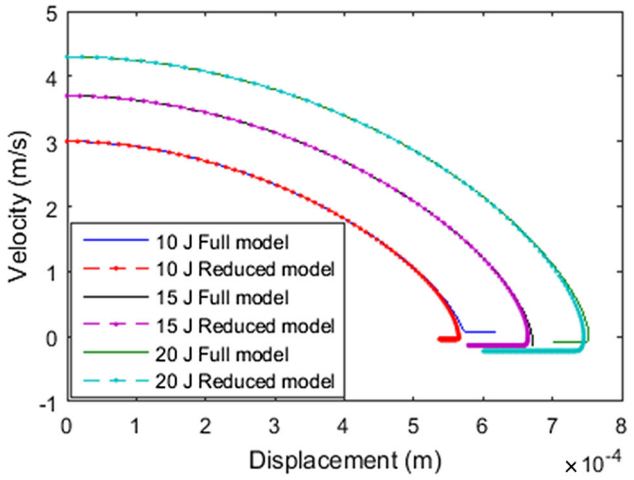

Fig. 12 Velocity–displacement curves of the model for different impact energy levels

Comparison between the full model and reduced model velocity–time curves for different impact energy levels is presented in Fig. 11. Good correlation is also achieved between the models during initiation and growth. It can be seen from the curves that during the 15 J impact energy test, a gradual decline in velocity from initiation to 0.178 and 0.106 m/s within a period of 0.33 ms is predicted for the full and reduced models, respectively. With the 10 and 20 J impact energy levels, comparable trends of decline in velocities are predicted for the models. Beyond these thresholds, the impactor bounces back at a constant velocity during loading where the energy absorbed by the plate is dissipated to the composite laminate in form of matrix cracking, fiber breaking and debonding of fiber–matrix interface. The threshold failure is occasioned by the bending response as the laminate absorbs impact energy in the form of flexural stresses.

Figure 12 shows a plot of predicted velocity–displacement curves for the two models at different impact energy levels. A semi-concave curve representing the damage response of the composite laminates is observed for all the models. During the 20 J impact energy test, the full model declines nonlinearly to about 0.78 m/s velocity through a displacement of 0.75×10^{-3} m. On the other hand, a gradual nonlinear drop of 0.67 m/s over a displacement of 0.74×10^{-3} m is noted for the reduced model. Similar and consistent tendencies are achieved via the 10 and 15 J impact energy levels. In comparing the models, no significant difference is observed among the models curvature. It can also be seen from the plot that the maximum displacement of the impactor increases as the impact energy increases. The impactor reaches the peak displacement value when the impact velocity becomes zero rather than reaching the peak value. The displacement of the impactor is much larger than the thickness of the laminates, which is due to the bending deformation of the composite laminates.

5 Conclusion

The applicability of cohesive interface elements based on surface-based cohesive contact model for damage prediction in composites with low-velocity impact is investigated. ABAQUS/Explicit software is adopted to build the numerical model. Cohesive interface constitutive model is incorporated in the model to activate damage at the debonding interfaces of adjacent layers under compressive impact loading. The intra-laminar and delamination damage models are explicitly executed in the finite element software ABAQUS using a user material subroutine VUMAT. Impact force as a variable of time and displacement is compared with the experimental and numerical data from reference to validate the present model. The impact damage characteristic of cross-ply composite laminate was discussed. A parametric analysis with respect to damage mechanisms for both full and reduced models at different impact energy levels of the quasi-isotropic composite laminate was presented. The impact damage variables of full and reduced models such as velocity, acceleration and displacement with corresponding impact energy levels were also detail discussed. An excellent agreement is achieved between the full and reduced models predictions as a result of the incorporation of cohesive interface elements in the damage model which activated delamination initiation and progression. The current model will be useful in future to study damage progression behavior in composite laminates with cluster or multiply layups under low-velocity impact conditions.

Acknowledgements The research is partially supported by the Innovative Foundation for Doctoral Candidate of Jiangsu Province, China (KYLX15_1049).

References

Bouvet C, Castanié B, Bizeul M, Barrau J-J (2009) Low velocity impact modelling in laminate composite panels with discrete interface elements. Int J Solids Struct 46:2809–2821

Bui Q (2011) A modified Benzeggagh-Kenane fracture criterion for mixed-mode delamination. J Compos Mater 45(4):389–413

Choi I-H, Kim I-G, Ahn S-M, Yeom C-H (2010) Analytical and experimental studies on the low-velocity impact response and damage of composite laminates under in-plane loads with structural damping effects. Compos Sci Technol 70:1513–1522

Feng D, Aymerich F (2014) Finite element modelling of damage induced by low-velocity impact on composite laminates. Compos Struct 108:161–171

Hosur MV, Adbullah M, Jeelani S (2005) Studies on the low-velocity impact response of woven hybrid composites. Compos Struct 67:253–262

Jang J, Sung M, Han S, Yu W-R (2017) Prediction of delamination of steel-polymer composites using cohesive zone model and peeling tests. Compos Struct 160:118–127

Khalili SMR, Soroush M, Davar A, Rahmani O (2011) Finite element modeling of low-velocity impact on laminated composite plates and cylindrical shells. Compos Struct 93:1363–1375

Kumar D, Roy R, Kweon J-H, Choi J-H (2016) Numerical modeling of combined matrix cracking and delamination in composite laminates using cohesive elements. Appl Compos Mater 23:397–419

Lachaud F, Espinosa C, Michel L, Rahme P, Piquet R (2015) Modelling strategies for simulating delamination and matrix cracking in composite laminates. Appl Compos Mater 22:377–403

Li X, Hallett SR, Wisnom MR (2008) Predicting the effect of through-thickness compressive stress on delamination using interface elements. Compos A Appl Sci Manuf 39:218–230

Liu P, Gu Z, Peng X, Zheng J (2015) Finite element analysis of the influence of cohesive law parameters on the multiple delamination behaviors of composites under compression. Compos Struct 131:975–986

Long S, Yao X, Zhang X (2015) Delamination prediction in composite laminates under low-velocity impact. Compos Struct 132:290–298

Lopes C, Camanho P, Gürdal Z, Maimí P, González E (2009a) Low-velocity impact damage on dispersed stacking sequence laminates. Part II: numerical simulations. Compos Sci Technol 69:937–947

Lopes C, Seresta O, Coquet Y, Gürdal Z, Camanho P, Thuis B (2009b) Low-velocity impact damage on dispersed stacking sequence laminates. Part I: experiments. Compos Sci Technol 69:926–936

May M (2015) Numerical evaluation of cohesive zone models for modeling impact induced delamination in composite materials. Compos Struct 133:16–21

Mitrevski T, Marshall IH, Thomson RS, Jones R (2006) Low-velocity impacts on preloaded GFRP specimens with various impactor shapes. Compos Struct 76:209–217

Olsson R (2001) Analytical prediction of large mass impact damage in composite laminates. Compos A Appl Sci Manuf 32:1207–1215

Sevkat E, Liaw B, Delale F (2013) Drop-weight impact response of hybrid composites impacted by impactor of various geometries. Mater Des 52:67–77

Shi Y, Soutis C (2016) Modelling transverse matrix cracking and splitting of cross-ply composite laminates under four point bending. Theoret Appl Fract Mech 83:73–81

Shi Y, Swait T, Soutis C (2012) Modelling damage evolution in composite laminates subjected to low velocity impact. Compos Struct 94:2902–2913

Shi Y, Pinna C, Soutis C (2014a) Modelling impact damage in composite laminates: a simulation of intra-and inter-laminar cracking. Compos Struct 114:10–19

Shi Y, Pinna C, Soutis C (2014b) Interface cohesive elements to model matrix crack evolution in composite laminates. Appl Compos Mater 21:57–70

Soliman EM, Sheyka MP, Taha MR (2012) Low-velocity impact of thin woven carbon fabric composites incorporating multi-walled carbon nanotubes. Int J Impact Eng 47:39–47

Xiao S, Chen P, Ye Q (2014) Prediction of damage area in laminated composite plates subjected to low velocity impact. Compos Sci Technol 98:51–56

Systèmes, S-D. ABAQUS/Explicit (2011a) Version 6.11-1. User Documentation Manuals

Systèmes, S-D. ABAQUS/Explicit (2011b) Version 6.11. User Manual. ABAQUS Inc, Providence, RI, USA

Zhang J, Zhang X (2015) An efficient approach for predicting low-velocity impact force and damage in composite laminates. Compos Struct 130:85–94

Zhang X, Bianchi F, Liu H (2012a) Predicting low-velocity impact damage in composites by a quasi-static load model with cohesive interface elements. Aeronaut J 116:1367–1381

Zhang X, Bianchi F, Liu H (2012b) Predicting low-velocity impact damage in composites by a quasi-static load model with cohesive interface elements. Aeronaut J 116:1367–1381

Zhang D, Sun Y, Chen L, Pan N (2013) A comparative study on low-velocity impact response of fabric composite laminates. Mater Des 50:750–756